The Thesis committee for Solaleh Khezri

Certifies that this is the approved version of the following thesis:

Evaluation of the Aquifer Storage and Recovery Pilot Project in Liwa Area, Emirate of Abu Dhabi, UAE

APPROVED BY

SUPERVISING COMMITTEE:

Supervisor: _____

Randall Charbeneau

_____

Rolf Herrmann

Evaluation of the Aquifer Storage and Recovery Pilot Project in Liwa Area, Emirate of Abu Dhabi, UAE

by

Solaleh Khezri, B.S.

Thesis

Presented to the Faculty of the Graduate School

of the University of Texas at Austin

in Partial Fulfillment

of the Requirements

for the Degree of

Master of Science in Engineering

The University of Texas at Austin

December 2010

Abstract

Evaluation of the Aquifer Storage and Recovery Pilot Project in Liwa Area, Emirate of Abu Dhabi, UAE

by

Solaleh Khezri, M.S.E.

The University of Texas at Austin, 2010

SUPERVISOR: Randall Charbeneau

Emirate of Abu Dhabi is located in an arid region, where the main source of fresh water is desalination plants. The vulnerability of desalination plants renders planning for an alternative source of freshwater essential. In this study the feasibility of aquifer storage and recovery in the Liwa area, in Emirate of Abu Dhabi, United Arab Emirates was investigated. Based on operational data collected from the pilot project, the model was set up and calibrated. The calibrated model was used to study the effect of various operational parameters, namely storage duration, pumping rate, screen location, multiple cycle operation and periodic recharge, as well as some aquifer characteristics factors: dispersion and salinity profile. This study can be utilized to optimize the operation of the Liwa ASR project.

Table of Content

List of Tables

List of Figures

Chapter 1

Introduction

1.1 Overview

United Arab Emirates is largely dependent on desalinated water as their main source of fresh water. However vulnerability of desalination plants to pollution, natural crisis, disruption caused by maintenance works or even war makes planning for an alternative source of fresh water crucial. A sustainable and cost-effective choice for reserve of fresh water is implementation of aquifer storage and recovery system (ASR), which includes the artificial recharge and storage of surplus desalinated water in an aquifer.

To select a location for an ASR pilot study, the preliminary study was carried out by Gesellschaft für Technische Zusammenarbeit (GTZ). A site suitability index was developed to account for various factors such as quantity and quality of available recharge water, topography, the quality of native ground water, aquifer thickness and hydraulic parameters. As a result of this analysis the northern Liwa area was selected .To investigate the feasibility and capacity of the aquifer storage and recovery system, as an alternative source of fresh water for emergency conditions, a pilot project in the Emirate of Abu Dhabi, United Arab Emirates, was conducted by GTZ. Observation data during each phase of the project, namely: infiltration, storage and recovery was gathered from observation wells drilled within the study area.

1.2 Objective

The objective of this project is to construct a hydrogeological model to simulate the ASR project carried out in the Emirate of Abu Dhabi, in order to evaluate the recovery efficiency of model under various scenarios to understand the effect of following operational and aquifer characteristic conditions:

- Long time storage
- Pumping rate during recovery
- Periodic recharge
- Multiple cycle operation
- Location of the screen
- Aquifer salinity and dispersion

Chapter 2

Literature Review

Aquifer Storage and Recovery (ASR) involves injection/infiltration of fresh water to an aquifer for later use. It is a more cost-effective and environmentally sustainable alternative to surface water storage.

The challenge addressed here is the storage of water in a saline aquifer .The density difference between the fluids causes the fresh water to float toward the top of the aquifer and allow the saline water to intrude the well and make the freshwater irrecoverable.

The storage of fresh water in saline aquifer was investigated by Esmail et al. (1967) and was concluded to be technically feasible in relative low permeability aquifer with high injection rate and short storage period.

In absence of density gradient the fresh water plume would be cylindrical surrounded by a buffer zone (mixed zone) caused by dispersion and molecular diffusion. However, in case of ASR in saline aquifer, the density gradient makes the vertical interface unstable and causes it to rotate, which reduces the recoverable water. This will be discussed in detail later.

Recovery efficiency is used to evaluate the success of an ASR operation. It is defined as the ratio of volume of recovered water to the water injected. However, this definition is sensitive to water quality restriction of the recoverable water, and therefore

could be subjective. Kimbler et al. (1975) assumed that the recovery will be terminated when the toe of the tilted interface reaches the bottom of the well. Based on this conceptualization, Ward et al.(2007) defined the unrecoverable water as "the volume in the conical plume outside the inner cylindrical of the interface." Subsequently, based on this concept the recoverability ratio is defined as:

$$R^* = \frac{\pi \varepsilon B r_{0.05,bottom}}{V_i}$$

where ε is porosity, B is the thickness of the aquifer, V_i is the volume of injected water and $r_{0.05,bottom}$ is the radius of the 5% isochlor at the bottom of the interface, which is an approximation for the position of the toe of the tilt.

Although this conceptualization is conservative, it can be used for qualitative comparison during any phase of an ASR project.

2.1 Density Effects during Injection

Ward et al. (2007) further studied the density effects in ASR. They divided the flow and transport during injection, storage and recovery in to two components; forced convection, caused by hydraulic gradient and free convection, created by the density gradient. They then defined the mixed convection ratio, as the ratio between the free to forced velocity as following:

$$V_{free} = \frac{K_z \bar{\alpha}}{\varepsilon}$$

where K_Z is the average vertical hydraulic conductivity, $\bar{\alpha}$ is the density difference ratio, and ε is porosity.

$\bar{\alpha}$, the density difference ratio, is defined as:

$\bar{\alpha} = \frac{\rho_{(Cs)} - \rho_0}{\rho_0}$ where $\rho_{(Cs)} = \rho_0 + 0.0007C_s$

$\rho_{(Cs)}$ is the density of seawater, ρ_0 is the fresh water density, and C_S is the salt concentration of seawater.

$V_{forced} = \frac{Qpump}{2\pi r_{ave}\varepsilon B}$

Q_{pump} is the injection rate, ε is porosity, B is the thickness of the aquifer, and r_{ave} is the fresh bubble radius:

$r_{ave} = \sqrt{\frac{Q_{pump}t}{\pi B\varepsilon}}$ where t is the duration of injection and other parameters are as defined above.

$M = \frac{Vfree}{Vforced} = \frac{2\pi r_{ave}B}{Q} K_z\, \bar{\alpha}$

Thus During injection, when the injection is slow enough that M>>1, the free convection dominates and the interface would be significantly tilted, whereas with the high injection rate that M<<1, the forced convection governs the flow and the effect of density can be neglected. These two scenarios are shown in Figure 2.1.

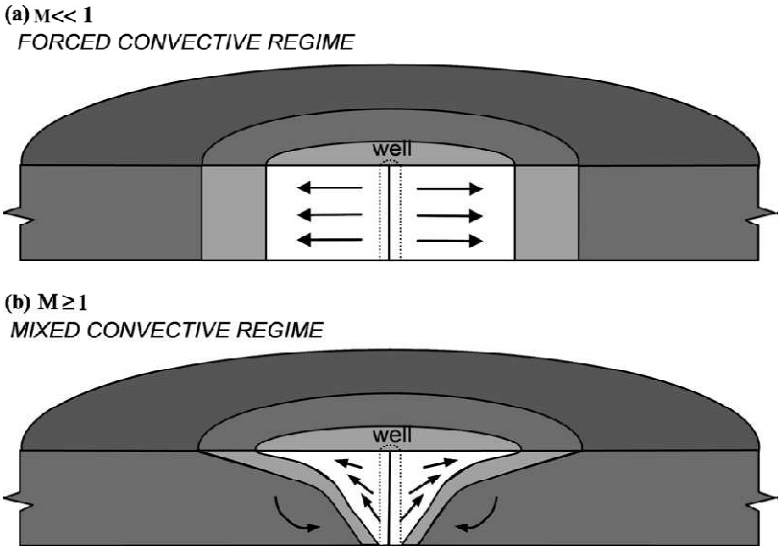

Figure 2.1: Concept of two convective regimes: (a) where forced convection greatly exceeds free convection, the interface will remain largely vertical (b) where both forced convection and free convection are of similar magnitude the result is a truly mixed convective regime. From Ward et al. (2007)

It can also be concluded that in addition to salinity, the pumping rate, hydraulic conductivity, thickness of the aquifer, influence the significant of interface tilting. It is contrary to some studies that define an ambient water salinity threshold as the main criteria for whether to account for the density difference (Missimer et al. 2002).

To observe the occurrence of density effect in a mixed convection zone a velocity ratio was introduced: $\frac{V_{bottom}}{V_{top}}$ for injection, and $\frac{V_{top}}{V_{bottom}}$ for recovery phase. It is expected that when the density effect are negligible this ratio would be 1, while smaller ratios would correspond to more significant density effects.

A numerical model was used to investigate the affect of various hydrogeological and operational variables on density effect during injection. As expected the low values

of M corresponded to the velocity ratio of 1 and the ratio decreased with increasing M; in cases with M>1 the velocity ratio was significantly reduced due to density effects . It was also observed that the higher dispersion diminished the density effects, as it reduces the density gradient between the fresh and salt water.

2.2 Density Effects during Storage

Ward et al. (2007) introduced the interface slope in order to measure the effect of density stratification during the storage, which is calculated as follows:

$$\theta = \frac{r_{0.5,top} - r_{0.5,bottom}}{B}$$

where $r_{0.5,top}, r_{0.5,bottom}$ are the radius to the 50% isochlors at the top and the bottom of the interface respectively ,and B is the thickness of the aquifer.

As expected, the density effects are dominant during the storage phase in the absence of convective forces. The effect of density variation coupled with the storage duration, and various dispersions was studied using numerical modeling. It was observed that as the storage time increases the volume of the recoverable water decreases, due to interface tilting. It is also seen that the rate of decrease in recoverable volume slows down with time. The physical explanation is that as the interface tilts toward the horizontal position, it becomes more stable and the tendency to tilt decreases. It was also detected that the rate of interface tilting is a function of width of mixed zone, as the wider mixed zones resulted in smaller interface slop over time, however it significantly reduced the recoverable volume; This phenomenon is explained as following: mixing decreases the

density gradient across the interface and reduces the free convection hence, the rate of interface tilting.

Another interesting observation was that cases with different hydraulic conductivity and density ratio but identical V_{free} had identical results, which confirms that density effects are equally affected by these two parameters. In cases that the density effects are insignificant, dispersion is the only parameter that controls the amount of recoverable water over time.

In order to study the relative contribution of dispersion and diffusion versus free convection, Raleigh number is defined by Ward et el. (2008):

$$\text{Ra}= \frac{K_{z,ave}\,\bar{\alpha}\,B}{(D_{d+}\beta_L V_{forced})\varepsilon}$$

where $K_{z,ave}$ is the average vertical hydraulic conductivity, $\bar{\alpha}$ is the density difference ratio, B is the thickness of the aquifer, D_d is molecular diffusivity, β_L is longitudinal dispersivity, V_{forced} is the idealized average velocity at the outer edge of the plume at the end of injection and ε is porosity.

At lower values of Ra dispersion dominates the convection during storage, while at the higher values density effects are more significant.

Ward et al. (2008) studied the effect of heterogeneity during storage. The hypothetical aquifer used for numerical modeling contained alternate layers of homogeneous and isotropic sediments of high and low hydraulic conductivity. As the

interface tilts in each layer the macroscopic interlayer tilting increases; in other words, the interface in lower layers migrates toward the wells, while in the upper layers, it moves away from the well, as shown in Figure 2.2. Once all the freshwater moves up the bottom layer, no freshwater can be recovered. At the microscopic level, the saltwater trapped in the low K layers starts to move downward contaminating the freshwater in the lower high K layer. On the other hand, the buoyant force of the freshwater, pushes the salt water from the lower K layer, toward the overlying fresh water; thus the freshwater is high K layer is contaminated by saltwater from both directions and is trapped in the low K strata, causing a significant reduction in the recoverable volume. Another possible phenomenon is the short circuiting of the saltwater into the well, driven by the high density of the saltwater pushing it from the bottom of the well.

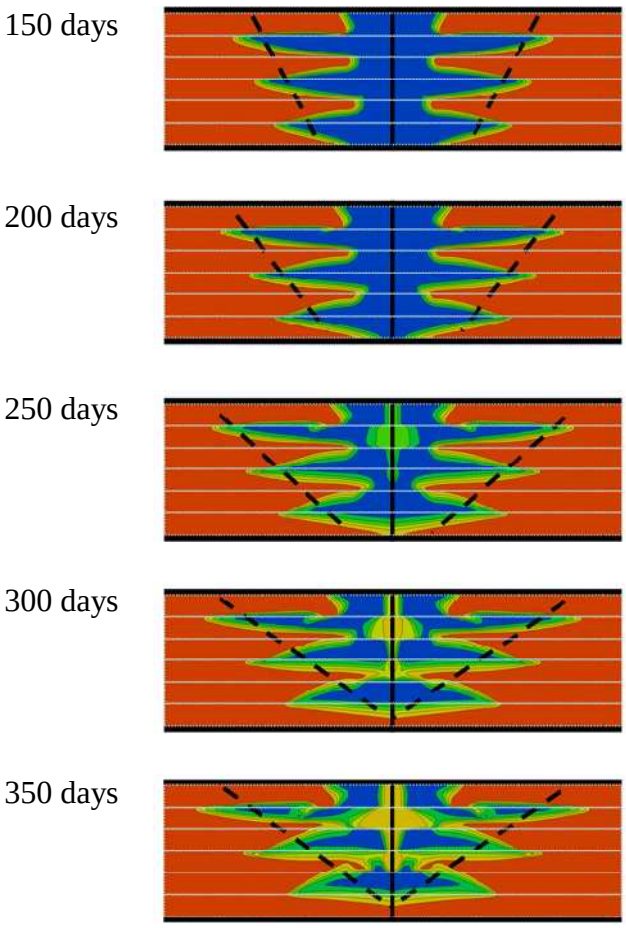

Figure 2.2: Concentration plots for a high density case ($\bar{\alpha} = 0.02$), K_2/K_1=10. The dark dashed lines denote inter-layer "macro-tilting". The pale line indicates the strata in the aquifer. Color regime C=0 (blue), C=28,571 (red).from Ward et al. (2008)

2.3 Density Effects during Recovery

The numerical modeling , performed by Ward et al.(2007), showed that high dispersion reduces the recoverable volume, loosing much of the water in the mixed zone, while decreases the effect of density. As expected when M<<1 and the system is advection dominant the velocity ratio is very close to 1, meaning that the movement of water toward the well is vertically uniform.; as M increase the density effect is more

significant which results in low velocity ratio. Interestingly, it is observed that with high M values the velocity ratio turns negative; in other words, while at the bottom the water is drawn to the well, it moves away from the well at the top, meaning that the free convection is so dominant that can't be overcome by pumping, this observation is consistent with different widths of mixing zone.

An examination of the breakthrough curves reveals that in low density cases there is a long period of freshwater recovery, followed by a gradual intrusion of ambient groundwater. In contrast, for higher density cases the breakthrough is observed much earlier due to interface rotation, and the rate of decrease of mixing ratio (amount of fresh water in recovered water) is very steep. However, as the dispersion starts to dominate the convection regime, they all converge to a common breakthrough curve.

A major issue in recovery of freshwater stored in a saline aquifer is the upconing of the saline water and subsequent contamination of recovered water. As the well screened in the freshwater discharges water, it also drives the underneath saltwater upward, causing saltwater upconing. Wirojanagud et al. (1985) discussed that up to a certain pumping rate which depends on the aquifer characteristics, a new equilibrium can be reached, creating a steady state cone shape interface between the two fluids. The interface moves further up as the pumping rate increases. A set of numerical simulations is performed using the conceptual model shown in Figure 2.3 based on the sharp interface method. The non-dimensional analysis of the results revealed that the interface rise (Z_{rise}/L) and the pumping rate have a linear relationship until Z_{rise}/L is about 0.35, beyond

which the rate of interface rise accelerates. There exist a critical pumping rate that creates a cone with the apex some distance below the well; however, any increase above this rate will make the interface unstable and saline water will flow to the well. The reason that the critical rise is at some distance below the well, is that any discharge rate greater than the critical value creates such a high gradient that the freshwater can no longer remain static.

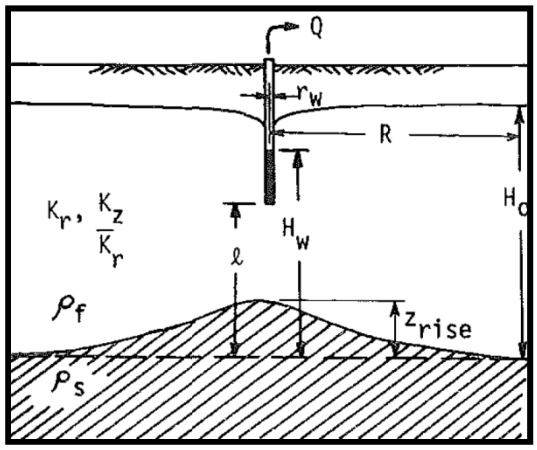

Figure 2.3: Conceptual model from Wirojanagud et al. (1985)

Reilly (1987) showed that in the more realistic density dependant model there is a partial salt discharge from the well even below the critical pumping rate. The amount of saltwater discharge would be a function of porosity and the dispersivity of the aquifer. However, a similar occurrence of sudden interface rise after a certain pumping rate is evident with the density dependant flow as well. A further investigation showed that the amount of salt water in the discharge is proportional to the pumping rate, though the slope of the concentration-discharge rate curve is steeper at the discharge rates greater than the critical rate determined by the sharp interface method, even when the screen is

simulated in different vertical positions. As expected, the location of the screen has a substantial effect on the critical pumping rate.

Saeed et al. (2003) evaluated the sensitivity of various aquifer characteristics, well design and operational parameters to saltwater upconing. In their study, hydrogeological and operational data were collected for 3 different locations with various well configurations in Indis basin in Pakistan. The calibrated model developed with MODFLOW and MT3D was used to carry out the study. Sensitivity analysis of aquifer characteristics showed that increase in vertical hydraulic conductivity and longitudinal dispersivity increased the salinity of discharged water while increase in horizontal hydraulic conductivity, effective porosity, specific storage and transverse dispersivity decreased the salinity of discharged water. The orders of sensitivity of aforementioned parameters are as follows:

Increase in salinity of discharged water: vertical hydraulic conductivity> longitudinal dispersivity.

Decrease in salinity of discharged water: horizontal hydraulic conductivity> effective porosity > specific storage > transverse dispersivity.

Furthermore, the dimensionless analysis of the numerical simulations revealed that the relationship between vertical hydraulic conductivity and longitudinal dispersivity with salinity of pumped water is almost linear, while horizontal hydraulic conductivity and effective porosity have a polynomial relationship with discharged water salinity. This

means that there is an optimum value for each parameter beyond which the salinity tends to stabilize.

Sensitivity analysis of operational parameters to salinity of discharged water reveals that increase in pumping rate and well penetration ratio both increase the salinity linearly in the order it is mentioned.

Wirojanagud et al. (1985) discussed the design and operational criteria for prevention of upconing in recovery wells, using the sharp interface approach. It is assumed that the independent parameters that characterize upconing are anisotropy ratio (K_z/K_r), horizontal hydraulic conductivity(K_r), freshwater density(ρ_s), density difference ($\Delta\rho$), H_0, l, R and r_w ,as shown in Figure 2.3. Using the Bucking π theorem, together with the analysis of numerical simulation results, the pumping rate at the critical interface rise, is found as following:

$$Q = \Pi_1 \frac{K_r H_0^2 \, (\Delta\rho/\rho_s)}{\ln (\frac{R}{H_0})}$$

where $\Pi_1$is a dimensionless factor, which can be read from Figure 2.4.

It can be concluded from Figure 2.4 that the optimum value for l/H_0 is about 0.8. Below this value, the critical pumping rate decreases as the vertical hydraulic conductivity increases, holding other parameters constant.

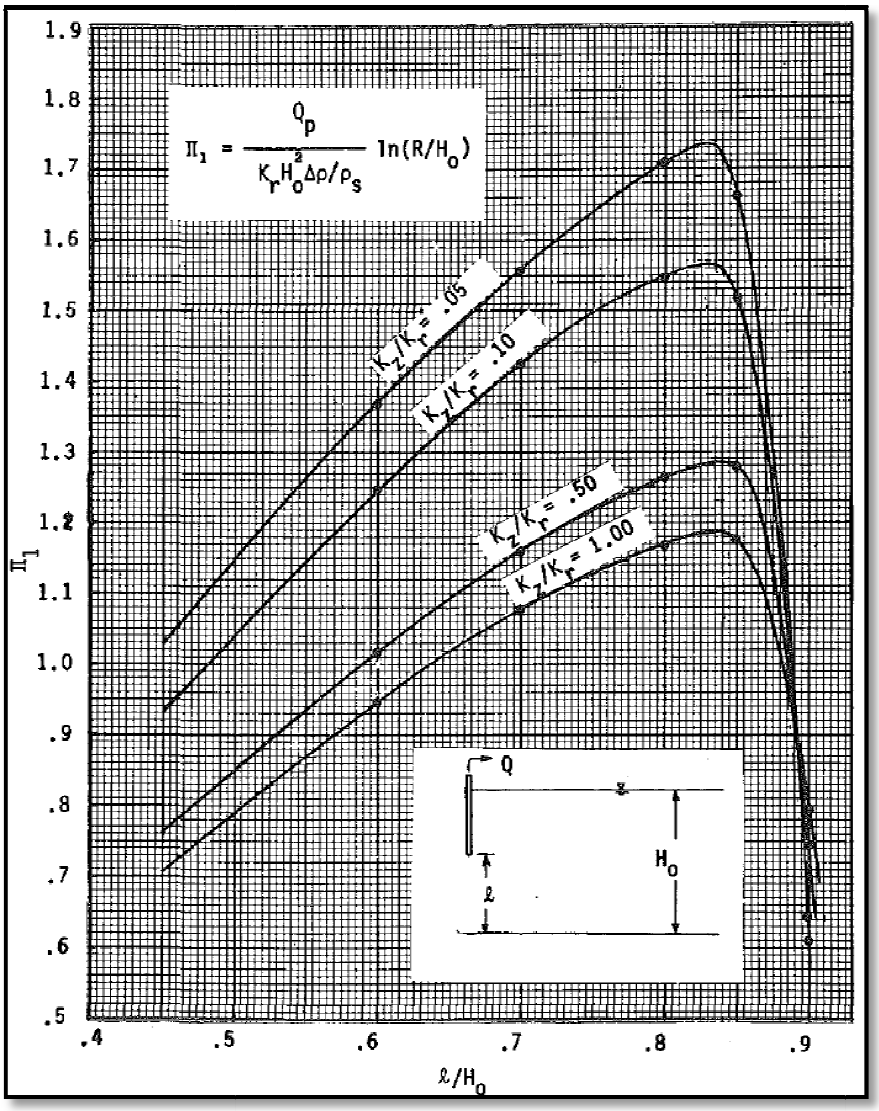

Figure 2.4: functional parameter relationships, from Wirojanagud et al. (1985).

2.4 Multiple Cycles Operations

Ward et al. (2007) showed that the recovery efficiency was improved with increase in the number of cycles. Also, as observed in each individual phase, dispersion attenuated the density affects; as the dispersion increased the result of density-invariant and density-dependent simulations get closer, however it yielded significantly lower

recovery efficiency, because of the increase in dispersive mixing in each cycle. The result also indicated that multiple cycles do not necessarily suppress the effect of density.

Ward et al. (2008) studied the behavior of a hypothetical heterogeneous aquifer, with alternate layers of homogeneous and isotropic aquifers of high and low hydraulic conductivity, through multiple cycles of ASR. It was revealed that a more heterogeneous aquifer demonstrated less macro-tilting during the storage. A highly heterogeneous aquifer retards the vertical mobility of the fluid, meaning it is not free to move from lower layers toward the top; hence yielding higher recovery efficiency as shown in Figure 2.5. However, even in a highly heterogeneous case, the saltwater continues to contaminate the injected plume over many cycles.

In conclusion, even a fast injection ($M<<1$) into a low density contrast aquifer, and after many cycles, there is still the possibility of significant reduction in recovery efficiency due to free convection.

End of Recovery K_2/K_1=10 K_2/K_1=100

Cycle 1

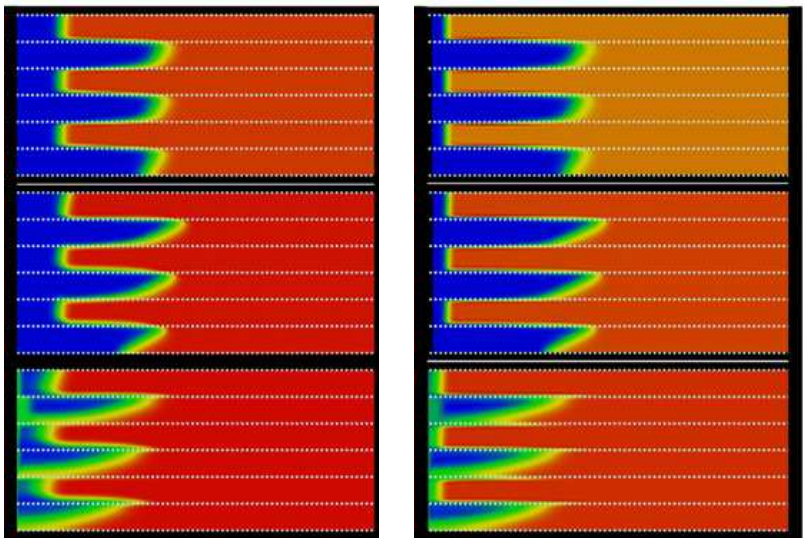

Cycle 10

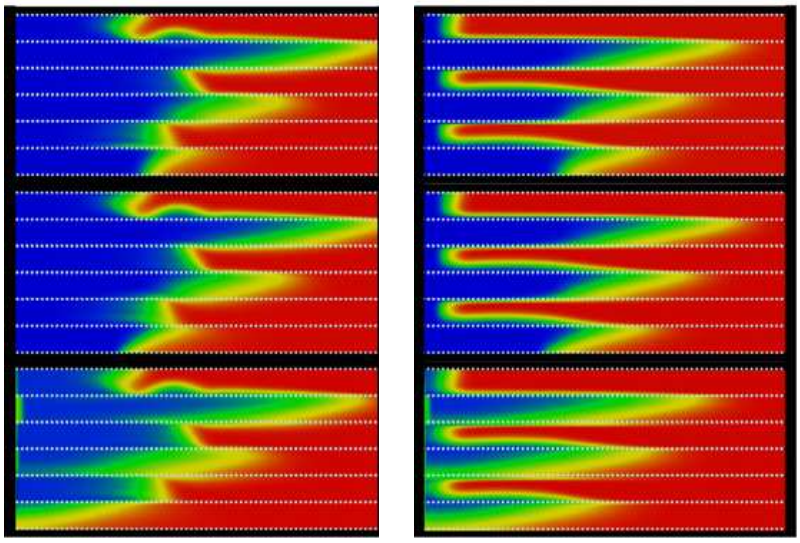

Figure 2.5: Concentration plots for the first and last cycle. Results shown are for K_2/K_1=1 and K_2/K_1=100, with low density ratio ($\bar{\alpha}$ =0.002). The pale line indicates the strata in the aquifer. Color regime C=0 (blue), C=28,571 (red).from Ward et al. (2008)

Chapter 3

Hydrogeological Characterization of Liwa Area

3.1 Lithology of the Northern Liwa

In the preliminary study performed by GTZ, a geo-database populated with information from 140 existing wells and 43 wells drilled particularly for the purpose of this project was used to assess the aquifer stratification. Since the water would be stored in the shallower aquifer most wells were less than 150 m deep, with only 4 boreholes drilled deeper than 490 m. Therefore less accurate hydrogeological information is available for the lower layer.

The two main stratigraphic units in the area are:

Quaternary Unit: Holocene and Pleistocene eolian fine to medium sand and interlunar deposits. The thickness of this unit varies from 100m to 150m, depending on the topographic elevation, and can be divided into two subunits. The upper unit is mostly composed of well sorted, fairly loose eolian dune sands with occasional appearance of find grained, slightly cemented interdunal deposits. These interdunal deposits are dominant in the lower subunit, which is composed of caliche horizons with traces of organic matter, silt stones, and even marls. The boundary between the two sub-units cannot be clearly defined by the information collected from the boreholes. However a significant increase in slightly cemented interdunal deposits in observed around 60 m above MSL. The formation below this depth does not have a significant contribution to

the ASR system due to its relatively low permeability, and thus is regarded as an aquitard.

Tertiary Unit: mudstone, evaporates and clastics of Miocene age. This unit is more than 360m thick. The upper subunit consists of mudstone layers and evaporates of the Lower Fars Formation. The lower subunit is characterized by prevalence of clastic sediment with layers of mudstone and anhydrite.

The boundary between the Quaternary and Tertiary unit (aquiclude) is defined by the first appearance of evaporates of the Lower Fars Formation, and is observed at a depth of 30m below MSL, and marks the end of aquifer/aquitard system. The Static groundwater level is encountered between 104m to 107m above MSL (Dawoud 2010).

Figure 3.1 shows the hydrogeological cross-section of the northern Liwa area.

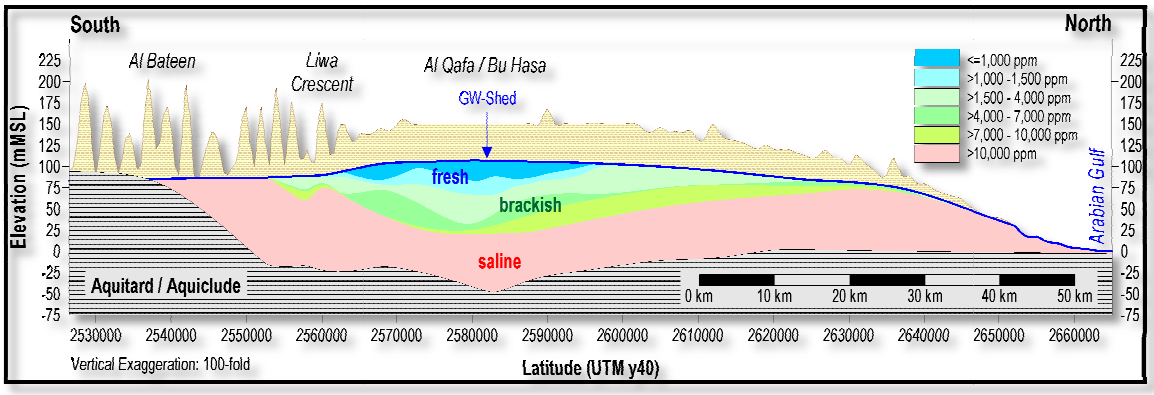

Figure 3.1: Hydro-geological Cross-section of Northern Liwa Area

3.2 Groundwater Flow

The study area is located within a major groundwater divide running from east to west, where the shallow to medium groundwater north of it flows to the north, toward the Persian Gulf, while the groundwater south of the divide flows to south toward Saudi Arabia. From the eastern half of the study area, groundwater flows with a maximum hydraulic gradient of 0.005% radial to adjacent area.

3.3 Hydraulic Character of Northern Liwa

In order to understand the geo-hydraulic character of the area, such as transmissivity, hydraulic conductivity, hydro-chemical composition and vertical salinity profile, 23 pumping tests were carried out. The geo-hydraulic conductivity calculated from the pumping tests varies between 2 m/d to 60 m/d with an average of 27 m/d and a median of 28 m/d. Transmissivity ranged from 100 m^2/d to 3000 m^2/d with an average of 1,065 m^2/d and the median of 950 m^2/d, where the lower values refer to the deeper part of the aquifer. In order to obtain the vertical hydraulic conductivity, one well infiltration and four tank infiltration tests were performed. The result of the infiltration test yielded in the infiltration rate of 11.8 m/d to 18.5 m/d. The vertical hydraulic conductivity calculated for the vadose zone ranged from 14 to 22 m/d.

3.4 Groundwater Quality

The evaluation of hydro-chemical composition of the native groundwater is based on 40 groundwater samples , 37 of which is collected after a long-term constant discharge

from the well, while the other 3 samples are derived by excavation where groundwater is very shallow. The analyzed Total Dissolved Solid (TDS) ranged from 348 ppm to 12,314 ppm (Dawoud 2010).

Figure 3.2 shows a profile of native water salinity in Electrical Conductivity (EC) where

TDS (mg/l) = 0.655 EC (µS/cm).

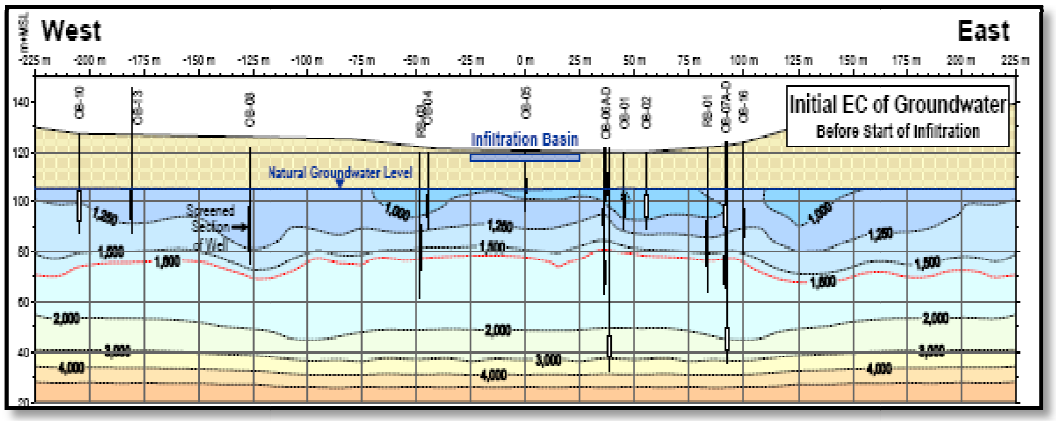

Figure 3.2: Profile of Native Water Salinity

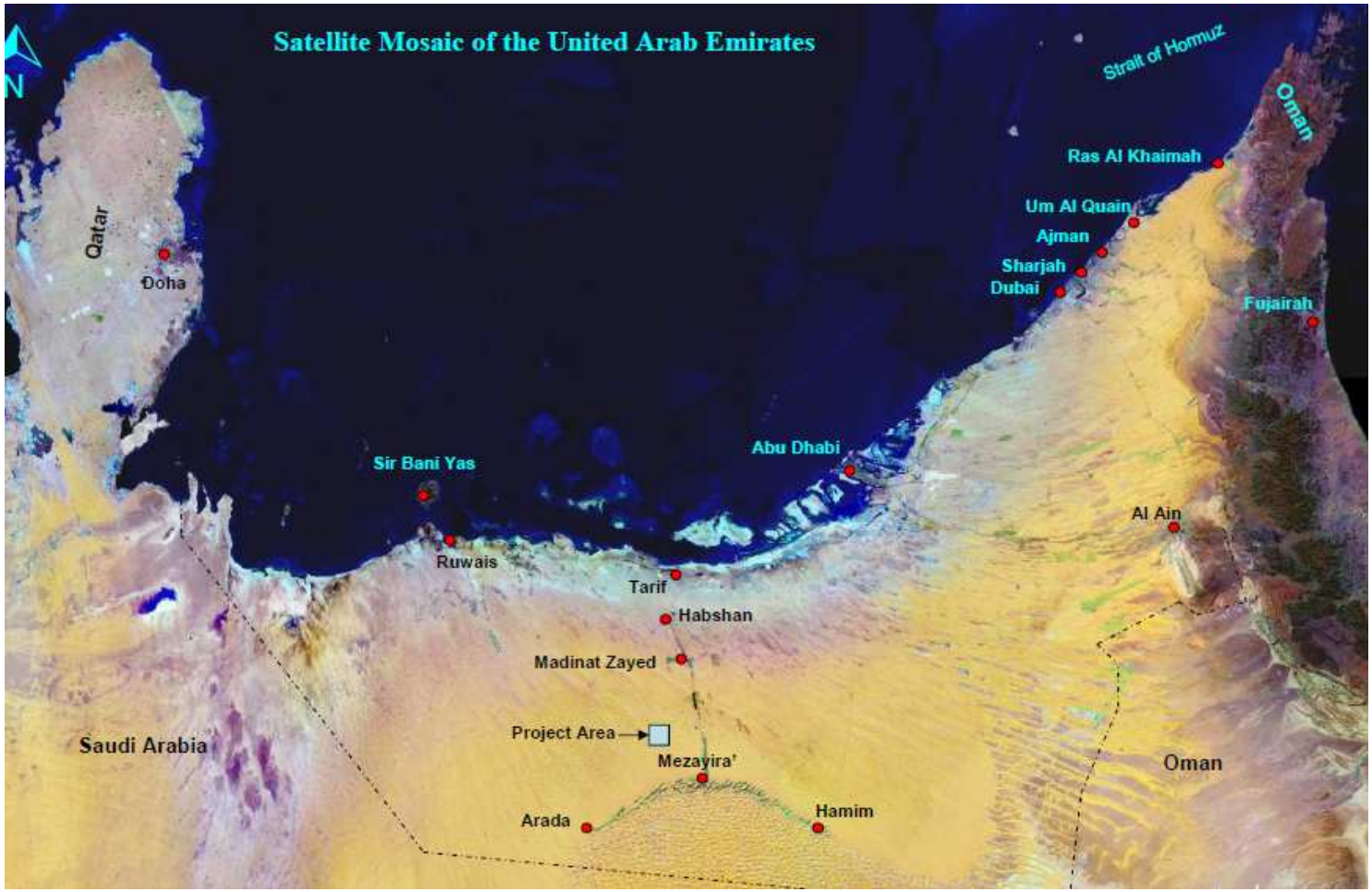

Figure 3.3: Location of the Project Area

Chapter 4

Construction of the Hydrogeological Model

4.1 Summary of the Liwa ASR Pilot Project

The pilot test was carried out by GTZ in northern Liwa area located about 230 km southeast of the City of Abu Dhabi. It included infiltration of desalinated seawater with 262 mg/l TDS at the rate of 250 m^3/h into a 60 m x 36 m infiltration basin for 250 days, which add up to about 1,500,000 m^3, followed by 48 days of storage, and was recovered at the average rate of 1495 m^3/d for 44 days, and then at 1093 m^3/day for 22 days from 4 production wells. Thus only 25% of water that was initially injected was recovered from the aquifer. Table 4.1 provides the detail schedule of the pilot project.

Table 4.1: Schedule of the ASR pilot project

Scheme Operation Mode	Operation Period			Abstracted Groundwater Volume during Period				Total Discharge Vol. at the end of period	DWS Surplus
	Start Date	Stop Date	duration	RB01 m^3	RB02 m^3	RB03 m^3	RB04 m^3	m^3	m^3
Infiltration	Oct-1	Jun-7	250	0	0	0	0	0	1,492,742
Storage	Jun-7	Jul-25	48	0	0	0	0	0	1,492,742
Continues abstraction	Jul-25	Sep-11	44	65,621	65,880	65,185	66,438	274,569	1,198,312
Continues abstraction	Sep-11	Oct-3	22	32,284	32,023	31,419	8	370,659	1,102,083

Recovery of the injected water was through four production wells RB01, RB02, RB03 and RB04 with a diameter of 0.66 m, which were located 55 m, 10 m, 18 m and 31 m away from the center of infiltration basin respectively and were screened from 74- 92 m MSL.

4.2 Conceptual Aquifer Model

The initial conceptual model consisted of 2 vertical zones. The upper layer extended from the water Table located at 105 m MSL to 60 m MSL. The average horizontal hydraulic conductivity of 20 m/d was assigned. The vertical hydraulic conductivity used was 8 m/d based on the 0.4 anisotropic factor reported by GTZ. The porosity was assumed to be 25%.

The lower layer expanded to -30 m MSL. The horizontal hydraulic conductivity was decreased to 3 m/d to account for the presence of silty layers. Based on anisotropy factor of 0.1 the vertical hydraulic conductivity of 0.3 m/s was assumed. The porosity was reduced to 0.1 due to occurrence of silty layers.

The properties of each zone are summarized in Table 4.2.

Based on observed temperature of 32°C the density of 995 kg/m^3 for freshwater and viscosity of 0.82 m Pa.s is used.

The salinity profile through the depth of the aquifer is as shown in Table 4.3 that is based on the cross section in Figure 3.2.

Table 4.2: Properties of the Conceptual Model

	Aquifer	Aquitard
Ground elevation	123 m MSL	
Groundwater level	105 m	
Aquifer depth (MSL)	105 m to 60 m	60 m to -30 m
Saturated thickness	45 m	90 m
Horizontal Hydraulic Conductivity	20 m/d	3 m/d
Anisotropy factor	0.4	0.1
Effective porosity	25%	10%

Table 4.3: Variation of saltwater concentration with depth

Elevation m	Electrical Conductivity µS/cm	TDS mg/l
105	1000	650
60	1800	1200
20	6000	4000
-30	10000	6550

4.2 Numerical Simulation

The aquifer is modeled in 3 dimensions using Eclipse H_20 that has the ability to model transport in vadose zone as well as the variation in density and salinity in the aquifer.

The model domain is 4 km x 4 km where the 500 m x 500 m ASR field is located at the center. The size of the model domain was selected to minimize the influence of the boundary conditions. The Model consists of 3 main horizons:

Top horizon: topographic map of the area.

Center horizon: steady-state water table.

Bottom horizon: bottom of the contributing zone.

The model consists of 32 blocks in x and y directions and 30 layers in the z direction. The first 10 layers represent the vadose zone with an average block depth of 6 m and 20 layers model the saturated depth of the aquifer with an average block depth of 13.6 m. The model is refined in the center, where the infiltration basin is located, as well as in the vicinity of the water table where the change in water table occurs during infiltration and recovery.

The grid was further refined to 60 vertical layers, however it did not show any improvement in the simulation result, therefore the coarser model was used because of computational time advantage. Figure 4.1 shows a 3-dimensional view of the grid, as well as distribution of horizontal hydraulic conductivity.

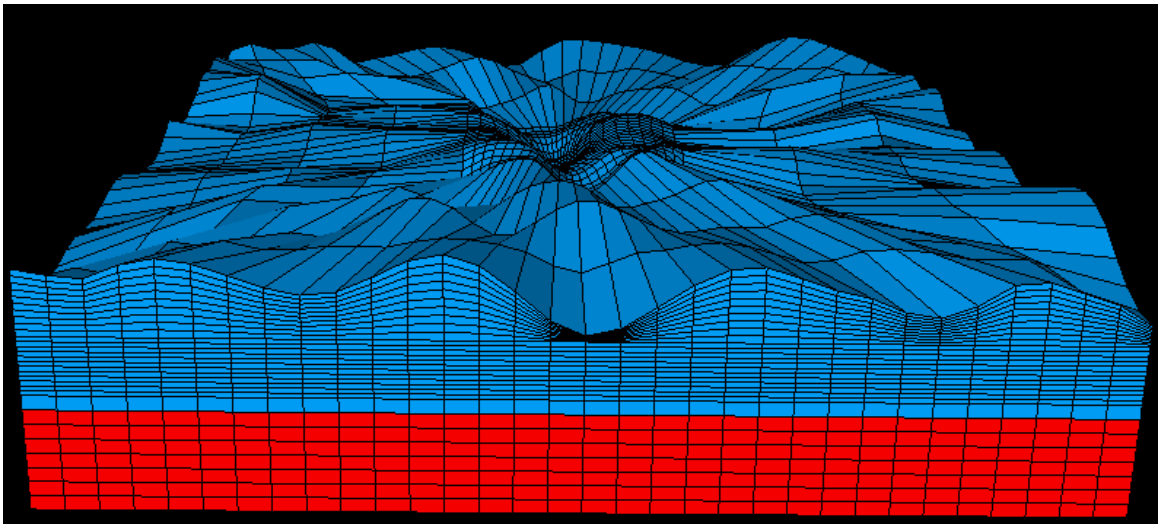

Figure 4.1: 3-D view of the Grid with 5 time vertical exaggeration, showing the distribution of horizontal hydraulic conductivity.

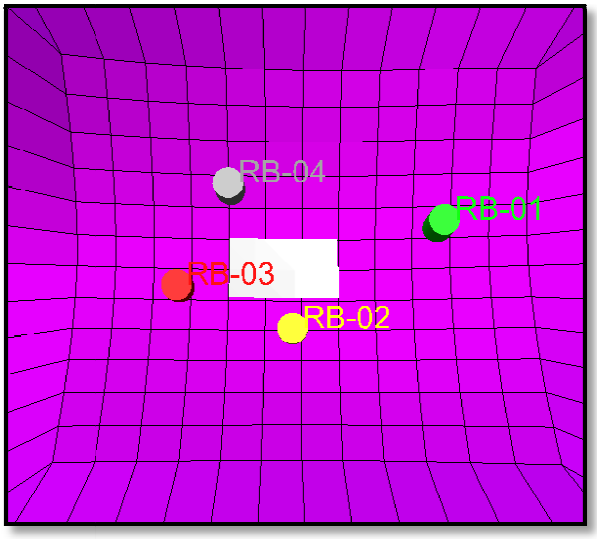

Figure 4.2: A zoom in to the center of the model showing the location of infiltration basin and the pumping wells. The cell size is 28.32 m x 15.35 m in the refined central cells.

4.4 Boundary Condition

A constant head boundary was specified at all four faces of the model to reproduce the condition at the aquifer. However, due to presence of native saline groundwater the head values decrease with elevation as the salt concentration and consequently density increases.

Table 4.4 shows the specified salinity and hydraluc head in selected saturated layers in the model.

Table 4.4: Properties for selected layers

Layer Number	Elevation (MSL)	Salinity	Density	Hydraulic Head
	m	gr/l	kg/m3	
11	103.13	0.672856	995.361641	105.073
15	88.13	0.856189	995.856085	105.078
20	69.38	1.085356	996.474141	105.068
25	31.88	3.1684	997.710252	105.027
30	-24.38	6.26338	999.564748	104.866

4.5 Steady State Condition

The steady state model is created to simulate the condition before the start of the pilot ASR project. The hydraulic gradient of 0.005% is ignored since the model is only run for reletively short duration, where the effect of such small gradient can be ignored, thus the steady state model is static. The criteria for steady state was set to maximum change of 1 mm in water level and 1mg/l TDS in brine concentration between 2 time

steps, which was reached after 19.22 days of simulation run. Figure 4.3 shows the salinity profile for the steady state model.

Figure 4.4 illustrates the change in hydraulic heads in selected blocks during the steady state simulation.

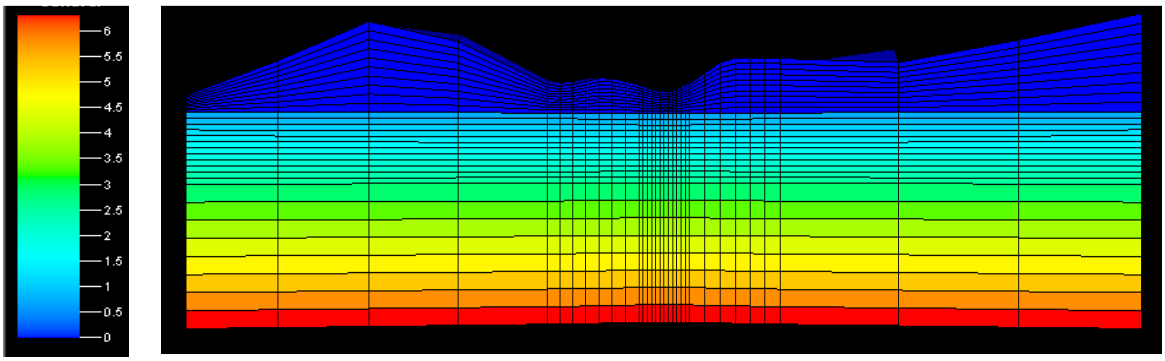

Figure 4.3: Salinity Profile at Steady State

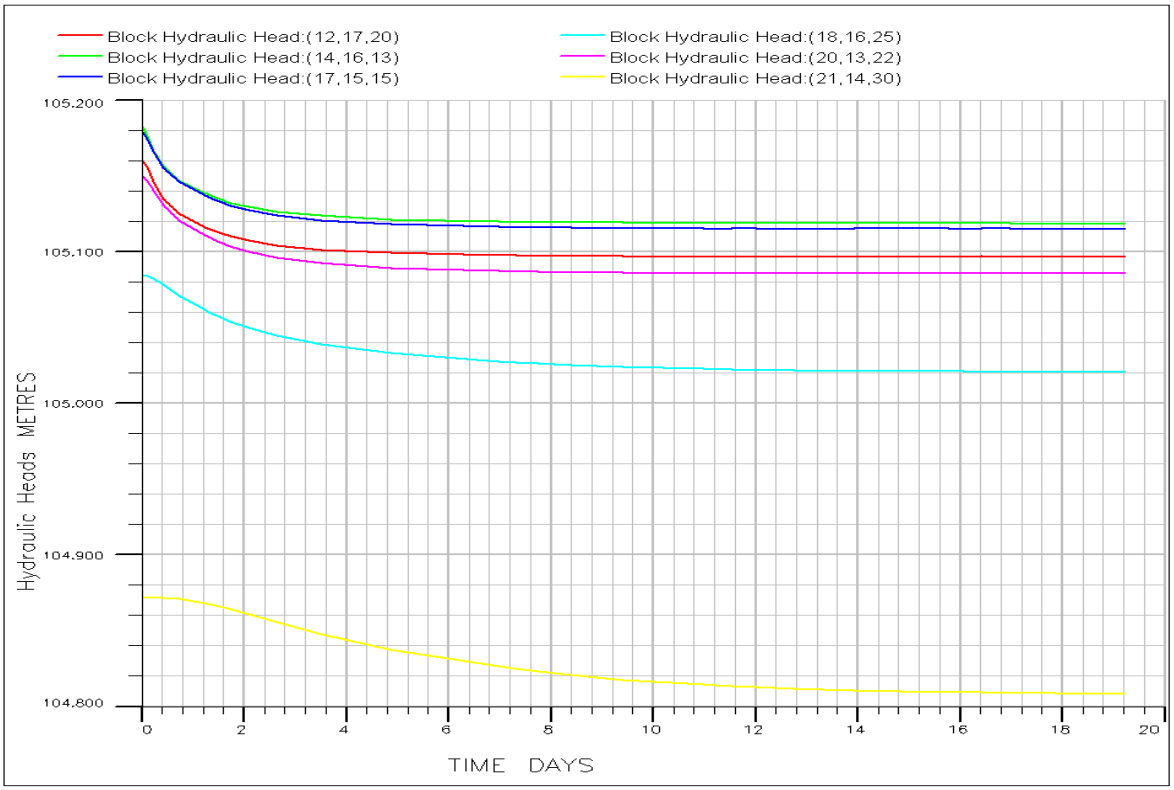

Figure 4.4: Hydraulic Head vs. Time for selected blocks in the model

4.6 Model Calibration

The simulation started with the conceptual model having 2 vertical zones. However, that model was unable to reproduce the change in hydraulic head observed in the wells during infiltration and recovery, with simulated result having less drastic change in hydraulic head, indicating that the actual porosity and hydraulic conductivity are less than estimated from the field test. The field data collected was mostly from the upper part of the aquifer so it was not certain in what depth the silty layers started to appear and how much it affected the hydraulic property of the aquifer. The final model consists of 3 layers, where the middle layer represents a transition zone from the sandy to

silty aquifer. The properties of the calibrated model are summarized in Table 4.5. The results of simulation and the associated error against the observed data are shown in Figure 4.5 and Table 4.6 respectively.

The saltwater concentration was verified against the observed salinity at each well at the end of recovery phase, as shown in Table 4.7.

The error in the calibration result is in range of 5% to 13% for the salinity data and at the maximum of 3% for the hydraulic head in the pumping wells, which is acceptable.

The calibrated longitudinal dispersivity for the model is 2 m, which is in line with the EPACML guideline. The estimated travel distance was determined, assuming a cylindrical freshwater plume, to be 150 m, thus based on the EPACML has a 60% probability to have dispersivity in range of 1-10 m. Due to the fact the model is homogenous in each zone, the assumption of 2 m dispersivity is justified.

Table 4.5: Properties of the calibrated model

	Aquifer 1	Aquifer 2	Aquitard
Groundwater level	105		
Aquifer depth (MSL)	105 m to 85 m	85 m to 45 m	45 m to -30 m
Saturated thickness (m)	20	40	75
Horizontal Hydraulic Conductivity m/d	12.5	12.5	0.4
Vertical Hydraulic Conductivity m/d	5	1.25	0.02
Effective porosity	0.2	0.1	0.05

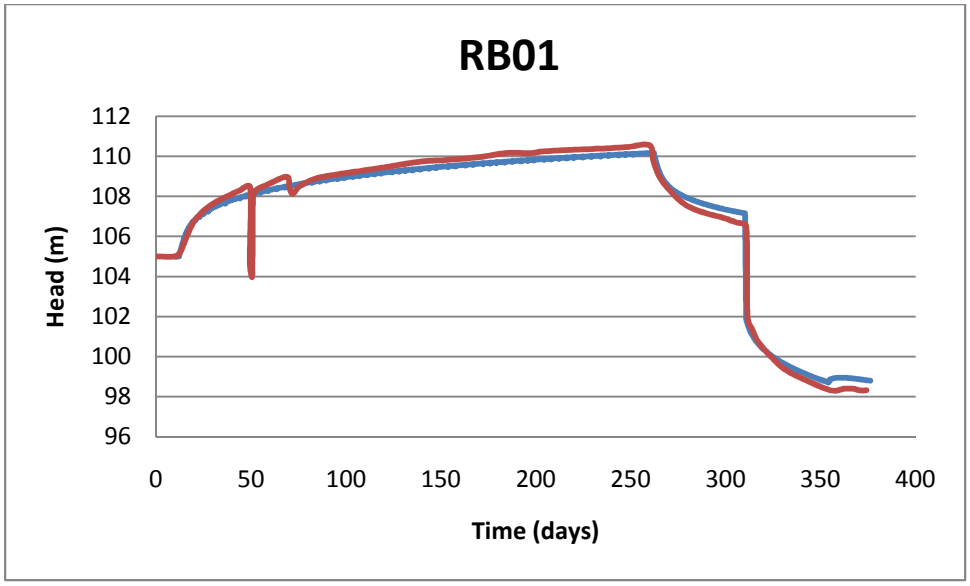
RB01
112
110
108
106
104
102
100
98
96
Head (m)
0
50
100
150
200
250
300
350
400
Time (days)

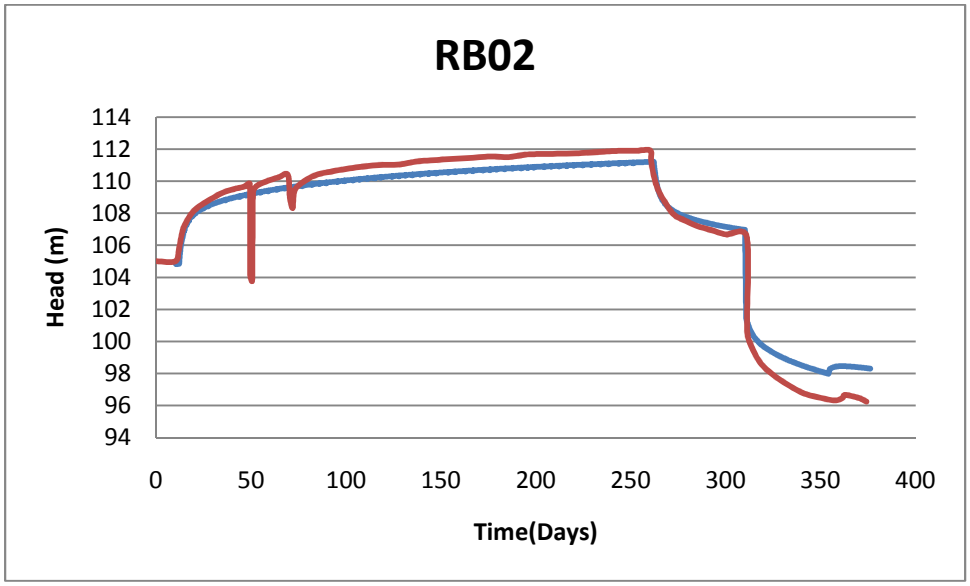
RB02
114
112
110
108
106
104
102
100
98
96
94
Head (m)
0
50
100
150
200
250
300
350
400
Time(Days)

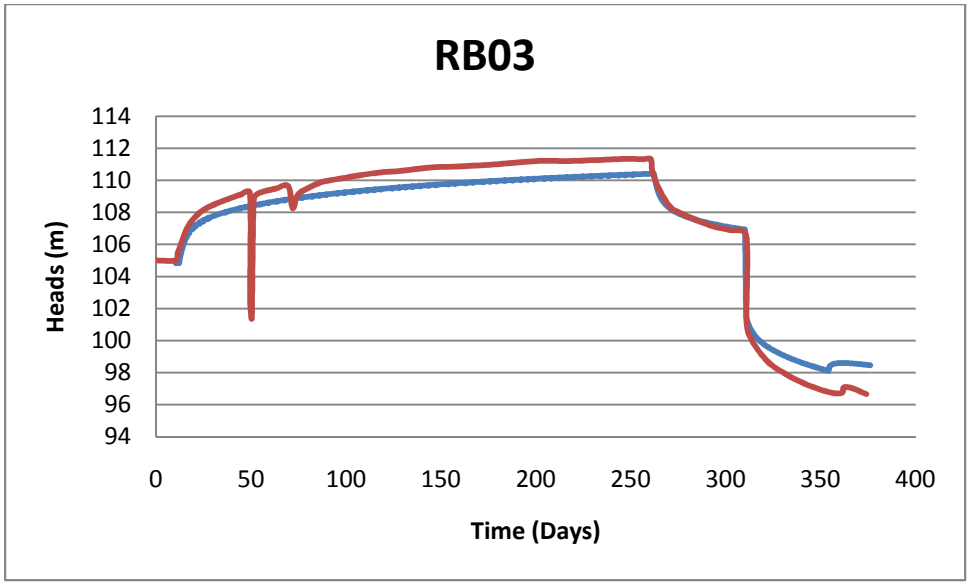

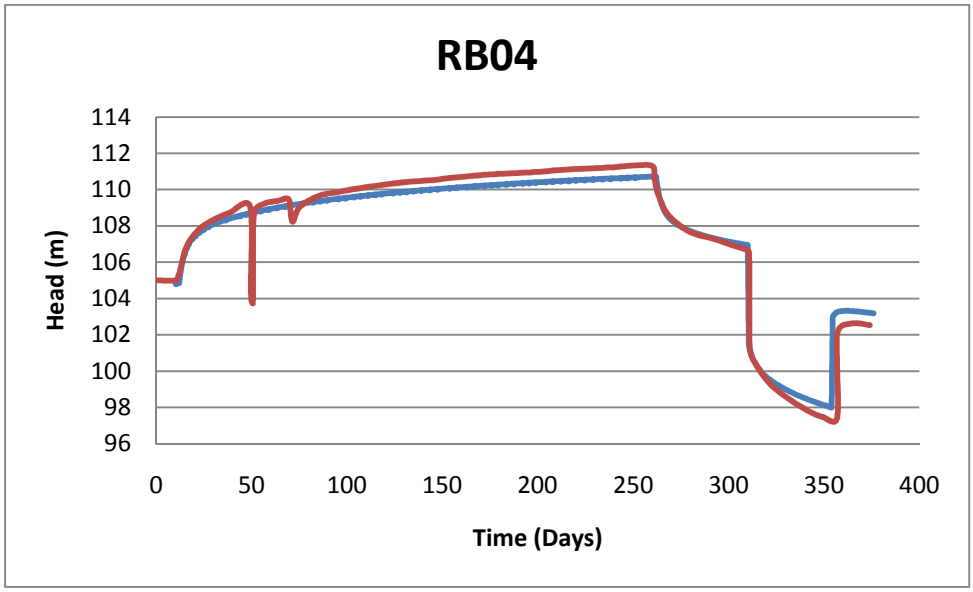

Figure 4.5: Hydraulic head observed at each well (red) against the simulation results (blue)

Table 4.6: Result of calibration of hydraulic head

	RB01	RB02	RB03	RB04
Max Head-simulated (m)	110.003	111.21	110.42	110.73
Max Head-Observed (m)	110.17	111.92	111.32	111.33
Error	0.15%	0.64%	0.81%	0.54%
Min Head-simulated (m)	98.32	96.25	96.66	102.52
Min Head-Observed (m)	98.80	98.317	98.47	103.18
Error	0.49%	2.15%	1.87%	0.64%

Table 4.7: Calibration of salinity in the wells

	Salinity Observed during the pilot test (mg/l)	Salinity Simulated (mg/l)	Error
RB01	350	320	8.57%
RB02	300	284	5.33%
RB03	310	289	6.77%
RB04	315	273	13.33%
Total	317	297	6.31%

Chapter 5

Model Evaluation and Prediction

In this chapter, the calibrated model was used to predict the ASR behavior under different operational and aquifer characteristic condition and optimize the recovery process.

The original model is further refined in the center of the grid domain, in x and y directions, in order to capture the shape and movement of the fresh water plume. The new grid consists of 50 blocks in x and y directions and 30 block in z direction. The refined center in the XY plane includes 40 blocks of 20m x 20m in each direction. The layering in the Z direction remained unchanged.

The infiltration basin is located in the middle of the top layer of the vadose zone and covers 9 blocks with the total surface area of 3600 m^2. The well design is changed to a symmetric configuration to facilitate the study of the model behavior. The well design includes a well in the center of the plume surrounded by 3 wells arranged in an equilateral triangle as shown in Figure 5.1.

Figure 5.1: Well field design

Various scenarios were simulated to understand the effect of the following parameters on recovery:

- Storage duration
- Pumping rate
- Screen location
- Multiple cycles
- Periodic Recharge
- Ambient groundwater density
- Dispersion of the aquifer

5.1 Storage Duration

In order to study the effect of storage duration on the recovery efficiency the following scenarios were simulated:

- Immediate recovery
- Recovery after 5, 10, 15, 20, 25, 30, 40 and 50 years of storage

The recovery efficiency was calculated for the threshold of 1000 mg/l salinity. Each well was shut off as the salinity of the discharge water exceeded the specified value; thus, the simulation would be terminated when either all the wells reached the salinity threshold of the pumped water or the total water production reached the infiltrated amount of 1,500,000 m^3, to assure that the aquifer will not be depleted.

The recharge water was infiltrated at 6000 m^3/day and was recovered at the rate of 16,667 m^3/day through the 4 wells, shown in Figure 5.1.

Figure 5.2 shows the movement of water plum under density gradient for 50 years of storage.

The salinity of water around the initial plume changes from 650 mg/l to 3000 mg/l; consequently the change in density is from 995.5 Kg/m^3 to 997.5 Kg/m^3.

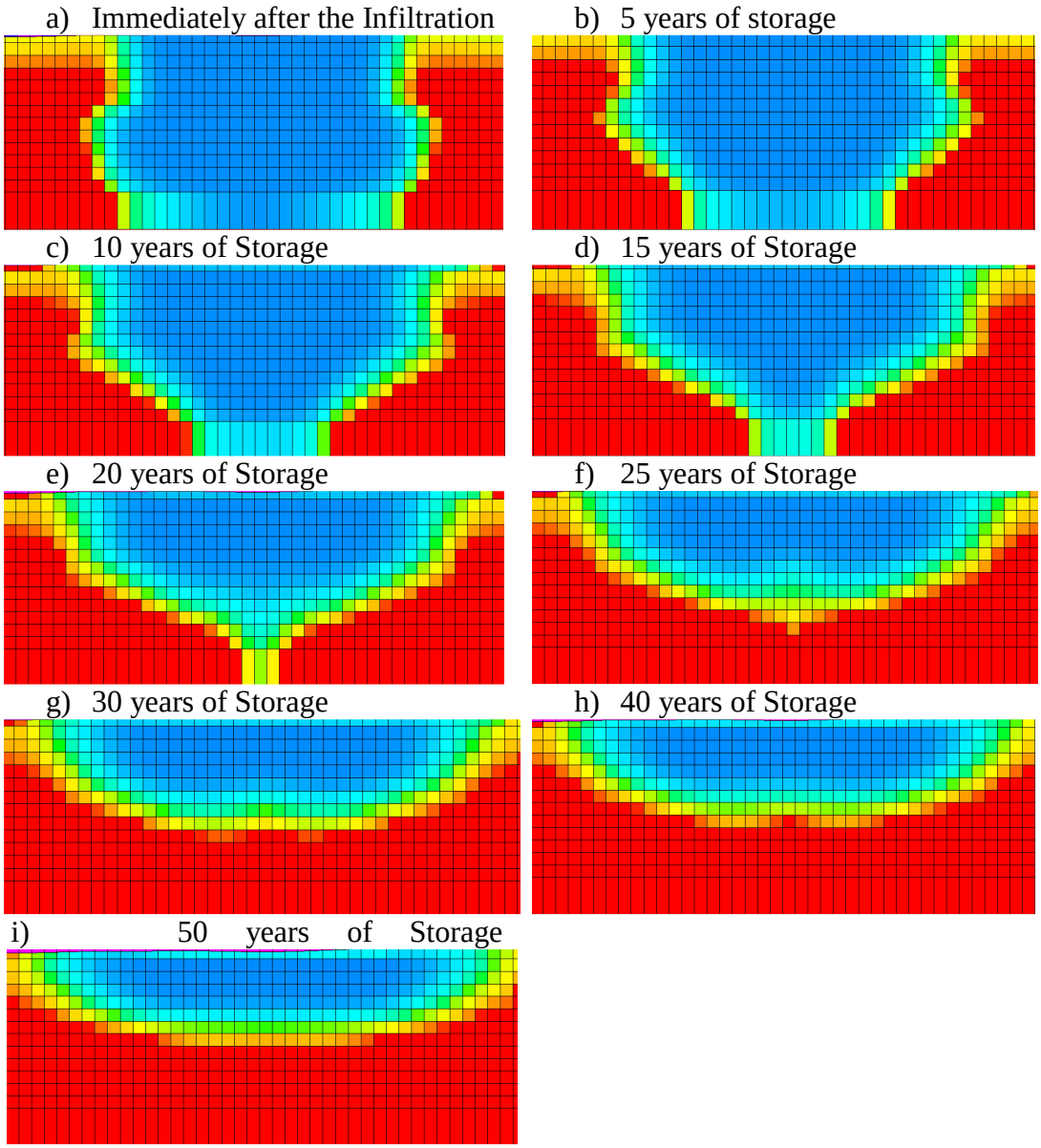

Figure 5.2: Movement of freshwater plume during 50 years of storage.

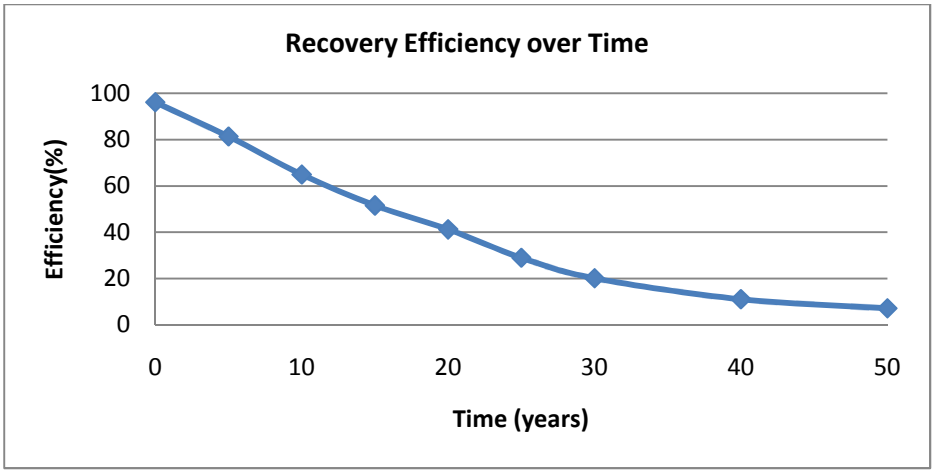

Figure 5.3: Recovery Efficiency versus Time

Table 5.1: Comparison of different storage periods

Storage Duration	Recovered Volume (m^3)	Terminated after	Efficiency
0 years	1,442,872 m^3	98 days	96.2%
5 years	1,221,146 m^3	73.6 days	81.4%
10 years	974,201 m^3	61.4 days	64.9%
15 years	773,741 m^3	48 days	51.6%
20 years	618,773 m^3	40.8 days	41.3%
25 years	434,818 m^3	29.4 days	29%
30 years	301,952 m^3	19.8 days	20.1%
40 years	166,128 m^3	11 days	11%
50 years	107,369 m^3	8.1 days	7.2%

The summery of the simulations' results are presented in Table 5.1. As seen in Figure 5.3, the change of recovery with time is almost linear for the first 30 years of storage; however, after 30 years the change in recovery efficiency with time is

significantly slower. This observation can be explained by transformation of the shape of the plume during the storage; as seen in Figure 5.2 (g-i) the freshwater plume is quite stable after 30 years of storage as it almost reaches the surface, and is subjected to much less density gradient and free convection forces.

5.2 Pumping Rate

Another operational parameter that was investigated is the pumping rate. In order to do so, the ASR system was simulated with different pumping rates for 2 storage scenarios as following:

- Immediate Recovery, with the rate of 750 m^3/day, 1000 m^3/day, 1500 m^3/day, 2083.33 m^3/day, 3125 m^3/day, 4166.66 m^3/day, 6250 m^3/day and 8333.32 m^3/day at each well and to the salinity threshold of 1000 mg/l
- 5 years of storage, with the rate of 750 m^3/day, 1000 m^3/day, 1500 m^3/day, 2083.33 m^3/day , 3125 m^3/day, 4166.66 m^3/day, 6250 m^3/day and 8333.32 m^3/day at each well and to the salinity threshold of 1000 mg/l

  First the effect of pumping rate on the salinity of discharged water was studied.

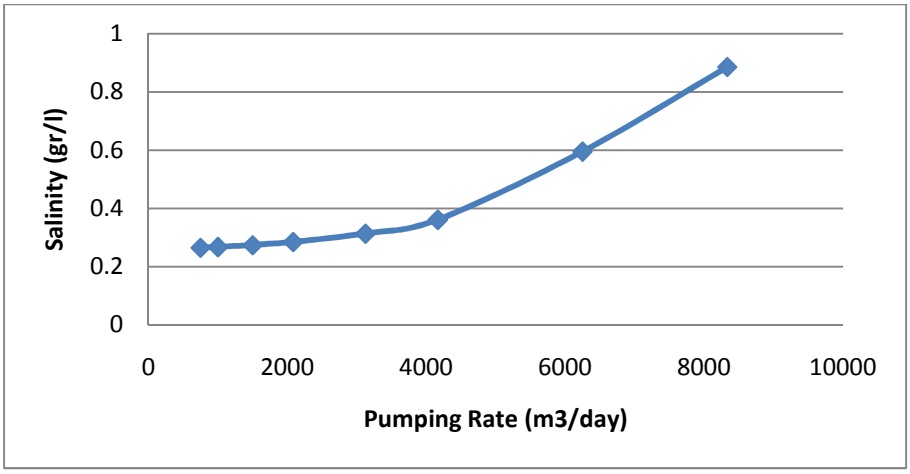

Figure 5.4: Change of salinity with pumping rate after 45 days of recovery

As reported by Wirojanagud (1985) and Saeed (2004) the salinity increases linearly up to a certain pumping rate, after which it increases at a greater rate. The critical pumping rate can be observed at around 4000 m^3/day.

However, of more interest is the change of recovery efficiency with pumping rate. Table 5.2 and Figure 5.5 show the result of simulations for the scenarios mentioned.

Table 5.2: Recovery efficiency versus pumping rate

	5 years of Storage		Immediate Recovery	
Pumping Rate (m^3/day)	Recovery Efficiency (%)	Recovered Volume (m^3)	Recovery Efficiency (%)	Recovered Volume (m^3)
8333.32	80.8	1211603.6	97.1	1456146.9
6250	80.6	1209095.3	96.9	1452961.6
4166.66	79.9	1198706.2	96.2	1442850.0
3125	79.2	1187500.0	95.6	1433677.9
2083.33	77.8	1166664.9	94.8	1421790.0
1500	76.4	1145777.9	94.1	1410900.0
1000	75.2	1127692.4	93.0	1394855.9
750	74.0	1110000.0	91.6	1374000.0

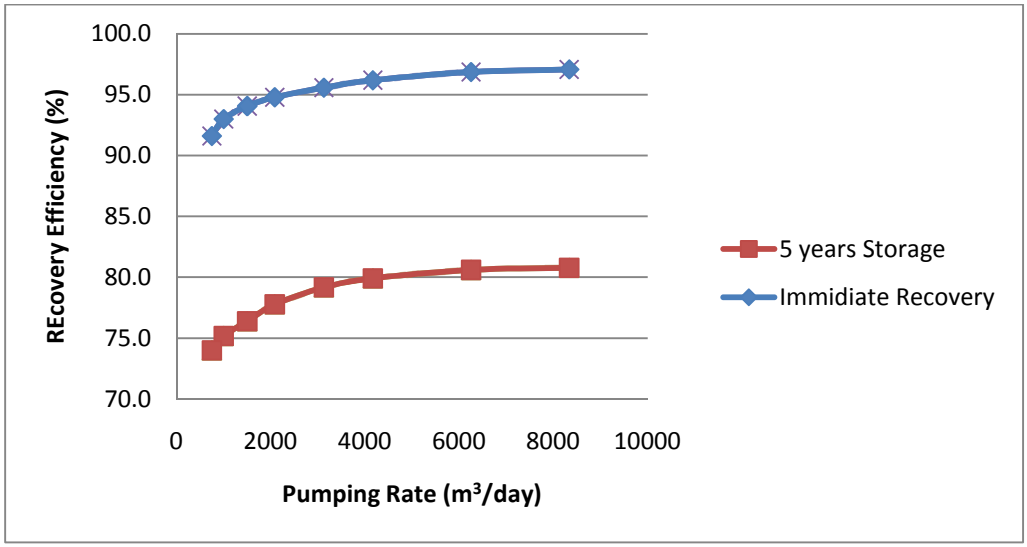

Figure 5.5: Recovery efficiency versus pumping rate

As observed in Figure 5.5, the recovery efficiency increases with increase in pumping rate, until it levels off and reaches the maximum practical recovery efficiency for the system. The phenomenon can be explained that as the pumping rate increases the pressure gradient at the well also increases, therefore the pump can draw freshwater from

further distance, hence raise the recovery efficiency. Also, the very low permeable aquitard underneath the freshwater bubble impedes the upward movement of the saline water from there; in addition, the relatively low vertical hydraulic conductivity counteracts the saltwater upconing. At last, less pumping rate and more recovery period allow more density dependent flow that as well reduces the recovery efficiency. Another interesting observation is that the system is quit insensitive to the pumping rate. When the pumping rate increases 11 fold the recovery efficiency increases by only about 6% in both cases.

In order to understand the effect of low vertical hydraulic conductivity combined with the underlying low permeability aquitard, the above scenarios were run in a homogenous aquifer, meaning that the vertical hydraulic conductivity in the upper aquifer and the hydraulic conductivities in the aquitard were increased to match horizontal hydraulic conductivity in the upper aquifer.

Figure 5.6 shows the end of recovery for different pumping rates for the heterogeneous and homogenous aquifers.

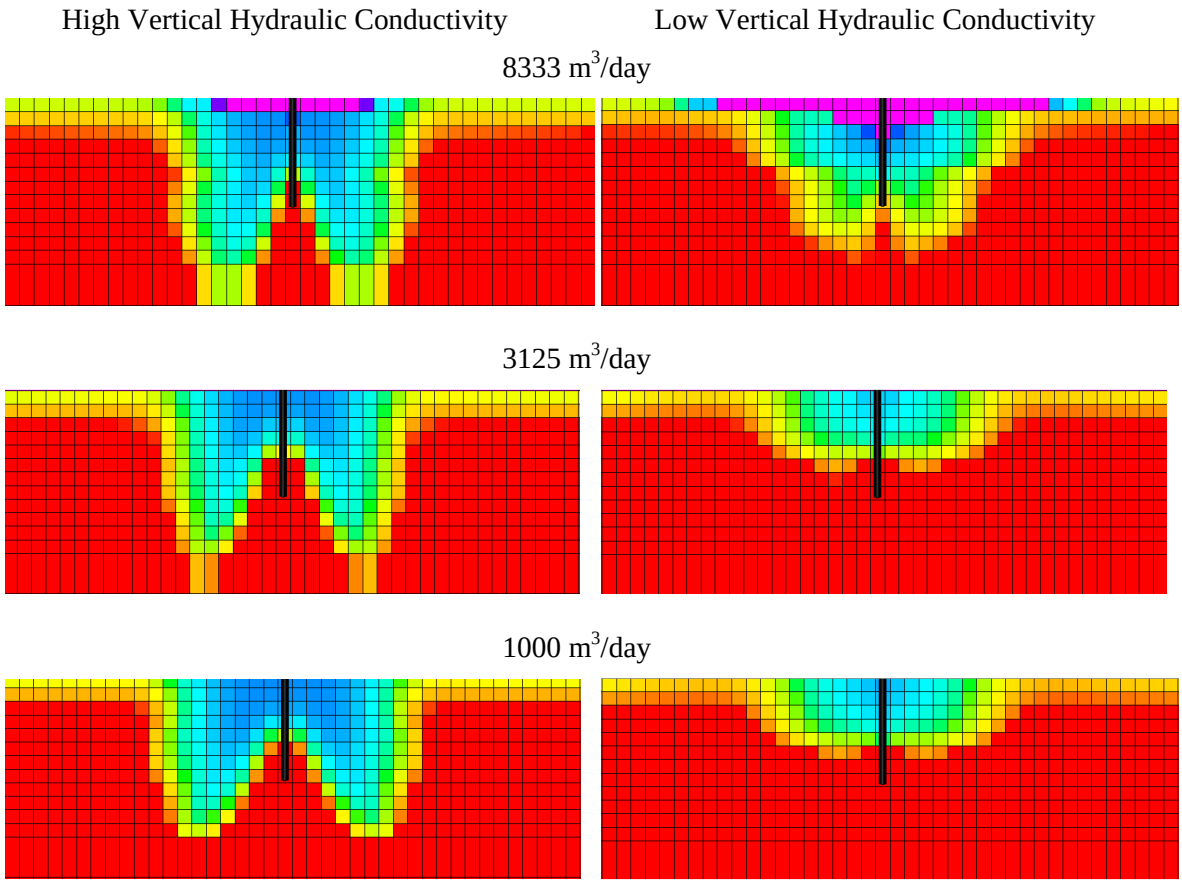

Figure 5.6: Upconing in homogenous (high vertical hydraulic conductivity) versus heterogeneous aquifer (low vertical hydraulic conductivity) with different pumping rates. Purple represents the cone of depression. Blue and red correspond to 260 mg/l and above 1000 mg/ respectively.

The upconing effect can be clearly observed in the homogenous, high vertical conductivity aquifer. As the pumping rates increases the saltwater upconing gets sharper. A slight saltwater upconing it only observed with the highest pumping rate in the heterogeneous, low vertical hydraulic conductivity aquifer.

Figure 5.7 shows the effect of saltwater upconing in the recovery efficiency.

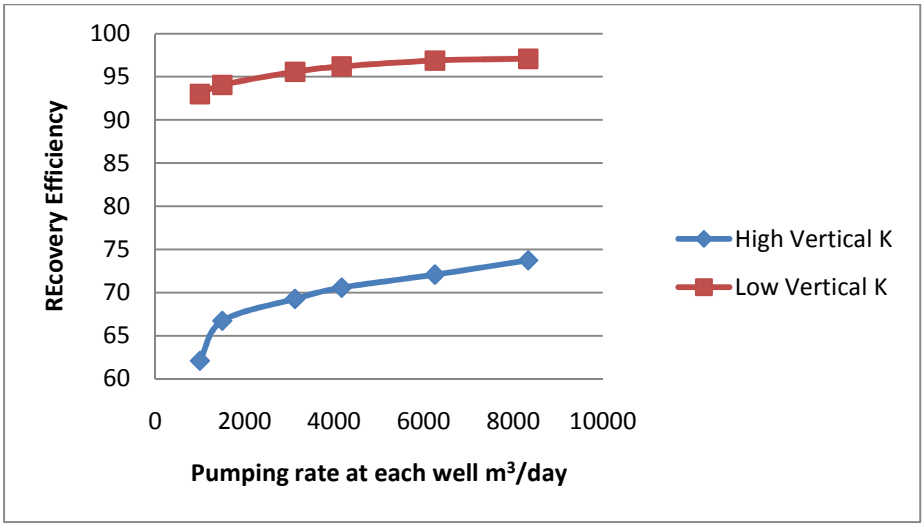

Figure 5.7: Effect of vertical hydraulics conductivity on upconing and recovery efficiency

It is evident that the upconing beneath the pumping well had a significant impact on the recovery efficiency and led to an early termination of recovery.

It should be noted that in the above simulations, a constant dispersivity is used.

5.3 Screen Location

In order to understand the impact of the screen location in the recovery efficiency scenarios with different screen location were simulated. In these scenarios the top of the screen was fixed at the water table and the length of the screen varied through the thickness of the freshwater plume.

Table 5.3: Screen Location versus Recovery Efficiency

Screen Length (m)	H_0 (m)	L (m)	L/H_0	Recovered Volume (m^3)	Recovery Efficiency (%)
11.25	33.75	22.5	0.666667	1006772	67.11813
15	33.75	18.75	0.555556	1006757	67.1171
18.75	33.75	15	0.444444	1003913	66.92751
22.5	33.75	11.25	0.333333	998550	66.57
26.25	33.75	7.5	0.222222	1003609	66.33327
30	33.75	3.75	0.111111	989809.1	65.98727
33.75	33.75	0	0	986231.5	65.74877

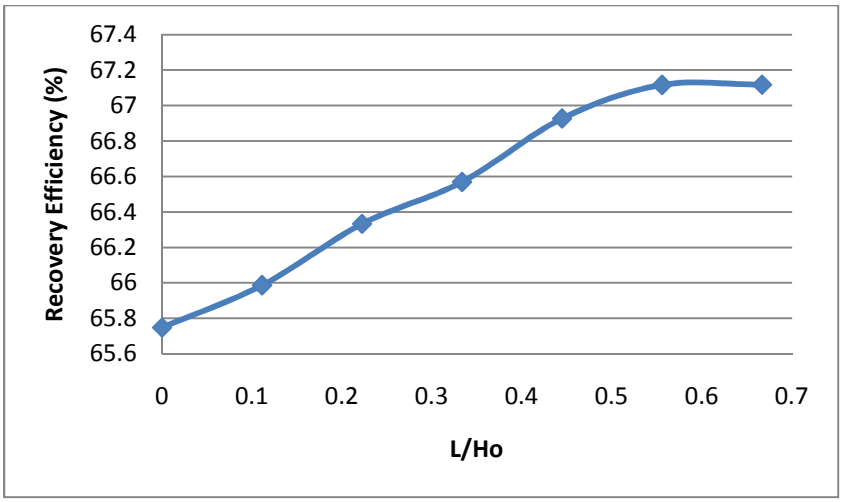

Figure 5.8: Screen Location versus Recovery Efficiency

As seen in Figure 5.8, the recovery efficiency proportionally increases with the penetration ratio (L/H_0), until it reaches an optimum values at L/H_0=0.667, which is reasonably close to the location of the optimum value reported by Wirojanagud (1985) to be around L/H_0=0.8; however the geometry of the aquifer did not allow for scenarios with greater penetration ratio.

5.4 Multiple Cycles

The impact of multiple cycle operation on efficiency of the ASR system was also studied. Each cycle consisted of infiltration of fresh water for 250 days, 1 year of storage, and recovery at the rate of 16,670 m^3/day through four wells. In each well, recovery was terminated once the salinity of discharged water reached 500 mg/l.

Table 5.4: Impact of Multiple Cycle Operation on Recovery Efficiency

No. of Cycles	Cumulative Recovered Volume (m^3)	Cumulative Recovery Efficiency (%)	Water Remained Under Ground(m^3)	Recovered in Each Cycle (m^3)	Cycle Recovery Efficiency
Cycle 1	910,763	60.7	589,237	910,763	60.7
Cycle 2	2,126,044	70.9	873,956	1,215,281	81.0
Cycle 3	3,462,442	76.9	1,037,558	1,336,398	89.1
Cycle 4	4,859,020	81.0	1,140,980	1,396,578	93.1
Cycle 5	6,284,018	83.8	1,215,983	1,424,998	95.0
Cycle 6	7,725,682	85.8	1,274,318	1,441,665	96.1
Cycle 7	9,182,712	87.5	1,317,288	1,457,030	97.1
Cycle 8	10,656,856	88.8	1,343,144	1,474,144	98.3
Cycle 9	12,136,020	89.9	1,363,980	1,479,164	98.6
Cycle 10	13,622,679	90.8	1,377,321	1,486,659	99.1

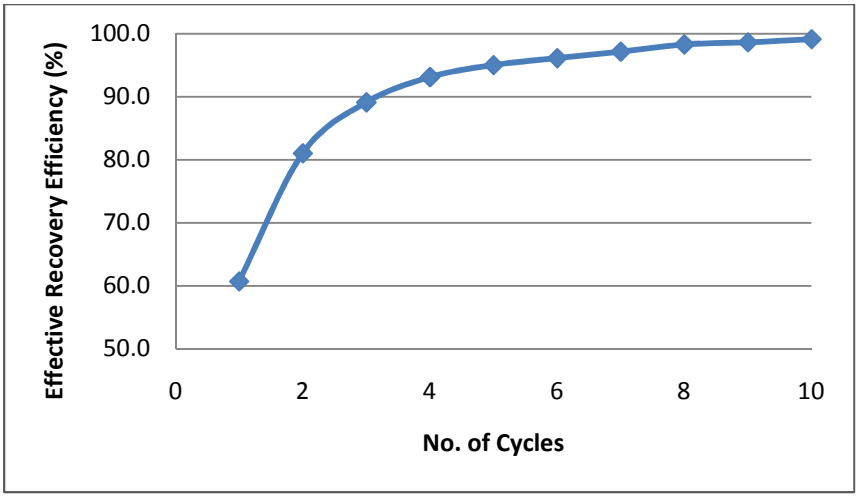

Figure 5.9: Impact of Multiple Cycle Operation on Recovery Efficiency

Two kinds of recovery efficiency are defined for multiple cycle operation: cumulative recovery efficiency which considers the fraction of total injected freshwater since the first cycle recovered up to the cycle of interest; and the effective recovery efficiency that disregards the volume of water that remained underground from the previous operations.

It is observed that after multiple cycles of operation the ASR system will almost reach 100% effective recovery even with one year of storage. It is also noticeable that in the second cycle of operation the recovery efficiency increased by 33%.

5.5 Periodic Recharge

In order to mitigate the significant loss of freshwater over long time storage, periodic recharge of the aquifer was proposed. In these scenarios, after the initial 250 days of infiltration, each year the aquifer was recharged for one month at the half of initial infiltration rate, 3000m^3/day, followed by 11 month of storage. Table 5.5 shows

the result of such scenarios for 5, 10, 15, 20 and 25 years of storage in comparison with the no recharge scenario.

Table 5.5: Comparison of periodic recharge with no recharge Scenario

Storage Time (years)	Volume of Water Stored (m^3)	Recovered Volume (m^3)	Efficiency with Recharge	Efficiency w/o Recharge
5	1,952,470	1,635,146	83.7%	81.4%
10	2,403,040	1,873,106	77.9%	64.9%
15	2,853,610	2,147,621	75.3%	51.6%
20	3,304,180	2,414,118	73.1%	41.3%
25	3,754,750	2,631,516	70.1%	29.0%

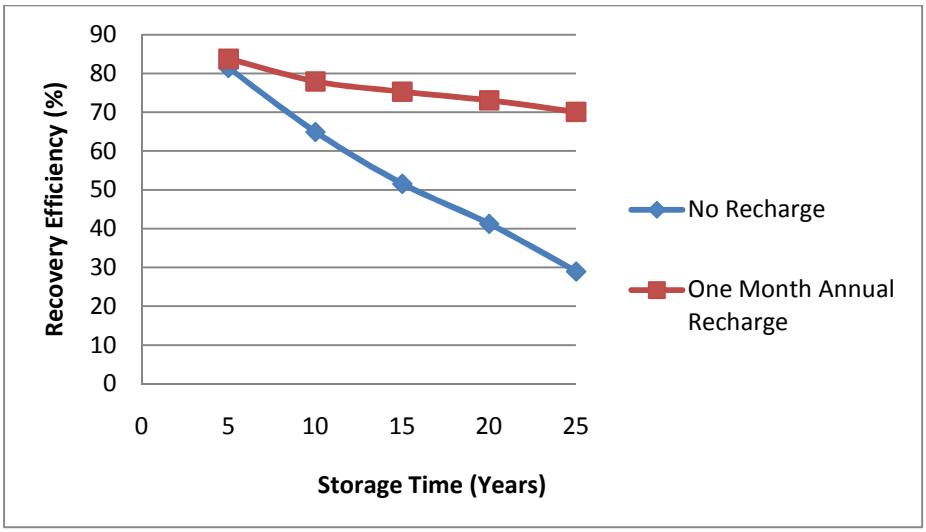

Figure 5.10: Comparison of periodic recharge with no recharge scenario

As expected and shown in Figure 5.10, the periodic recharge makes a noticeable positive impact on the performance of the ASR system with long time storage; as the storage period increases the effect is more evident.

The two following sections discuss the influence of aquifer characteristics on recovery efficiency.

5.6 Dispersion

In order to understand the effect of dispersion on the storage duration and recovery efficiency, the simulation scenarios mentioned in Section 5.1 were performed with 10 fold increase in dispersion for 0, 5, 10, 15 and 20 years of storage.

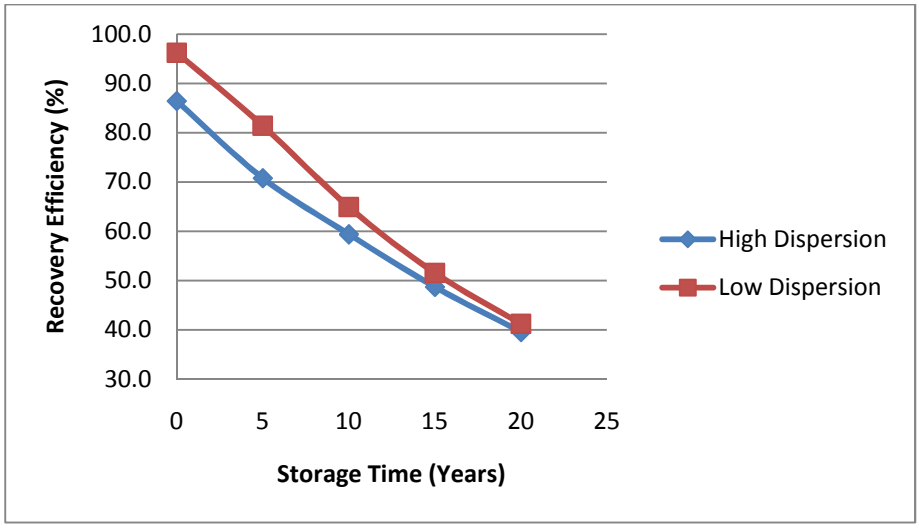

Figure 5.11: Impact of Dispersion on Recovery Efficiency

Table 5.6: Impact of Dispersion on Recovery Efficiency

	Low Dispersion		High Dispersion	
Storage	Recovered Volume (m^3)	Efficiency	Recovered Volume (m^3)	Efficiency
0 years	1,442,872	96.2%	1296414.3	86.4%
5 years	1,221,146	81.4%	1061955.6	70.8%
10 years	974,201	64.9%	891285.88	59.4%
15 years	773,741	51.6%	731094.69	48.7%
20 years	618,773	41.3%	594024.75	39.6%
25 years	434,818	29%		

As expected, the aquifer with higher dispersion has a less recovery efficiency at each storage duration. However, the more interesting trend, shown in Figure 5.11, is the diminishing impact of dispersion as the storage time increases. After 15 years of storage the effect of 10 times larger dispersion is negligible. Therefore, for the purpose of long time storage the dispersivity of the aquifer is not a parameter of concern, while for a short storage period it can have a significant impact on the recovery efficiency.

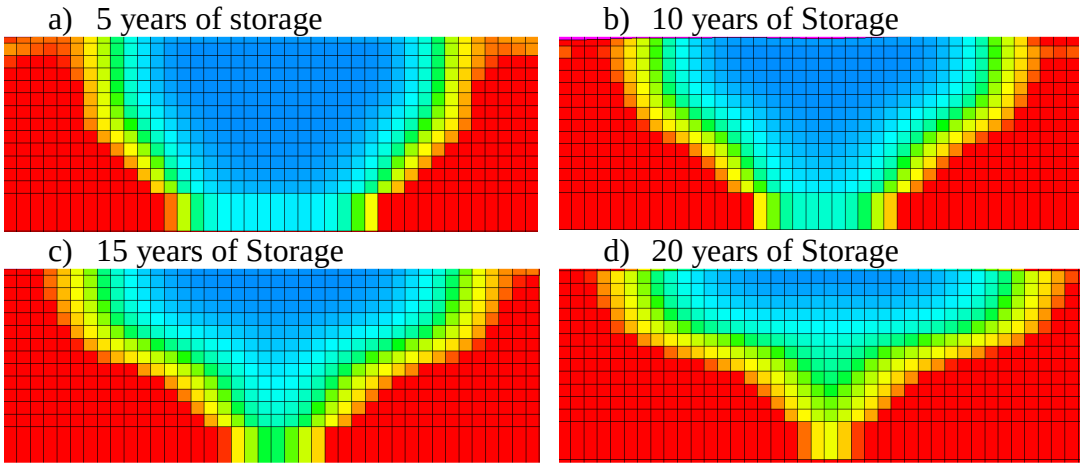

Figure 5.12: Movement of freshwater plume during 20 years of storage with high dispersion. The much thicker transition zone is evident in comparison to Figure 5.2.

5.7 Density Profile

The feasibility of aquifer storage and recovery in other areas of emirate of Abu Dhabi was investigated. Moving from inland toward Persian Gulf, salinity changes from less than 1000 ppm to about 100,000 ppm at the coast. In this study two different salinity profiles for density stratified aquifers were simulated for 5, 10, 15 and 20 years of storage. The recovery was terminated as the salinity of the pumped water reached 1000 ppm. The two density profiles included changing from 650 ppm to 10,000ppm and from 650 ppm to 30,000 ppm over 135 m thick aquifer.

Figure 5.13 shows the influence of salinity changes on the recovery efficiency of the system.

Figure 5.14 shows the movement of freshwater plume over time with different salinity profiles.

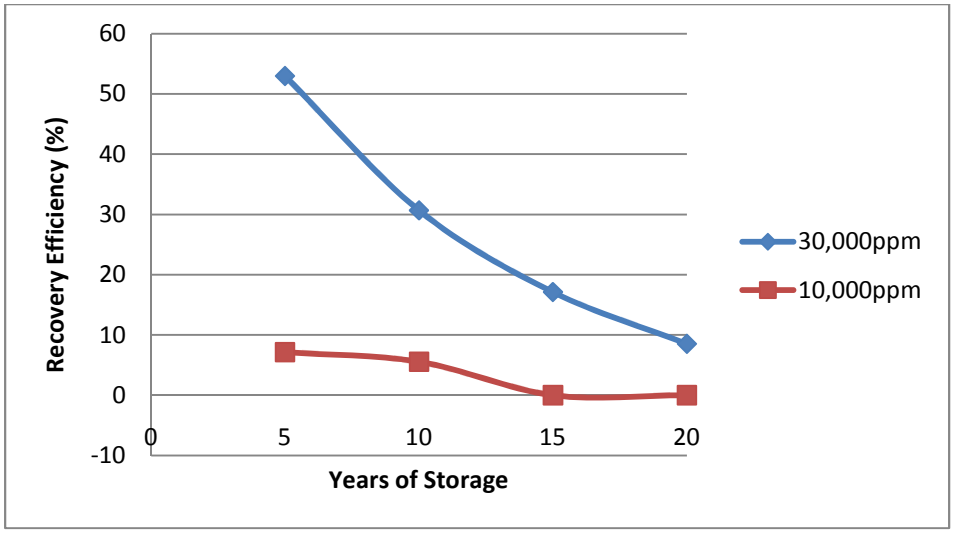

Figure 5.13: Change in recovery efficiency with various salinity profiles

650 ppm to 10,000ppm 650 ppm to 30,000

5 years of storage

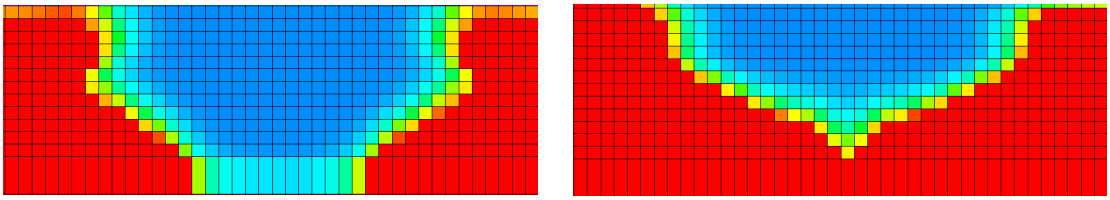

10 years of storage

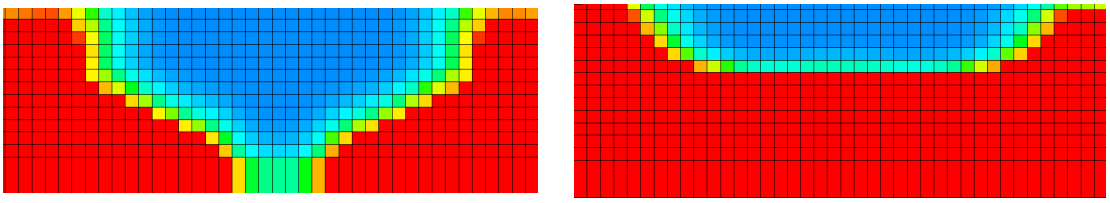

15 years of storage

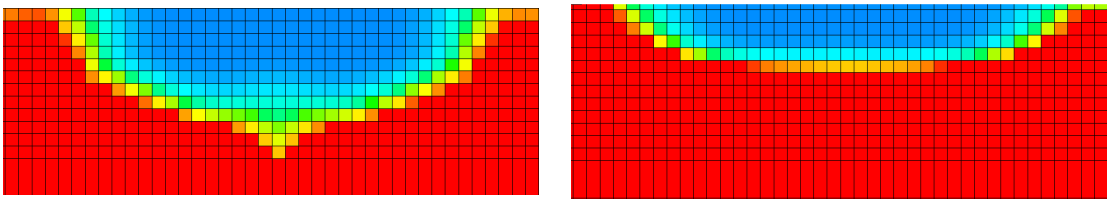

20 years of storage

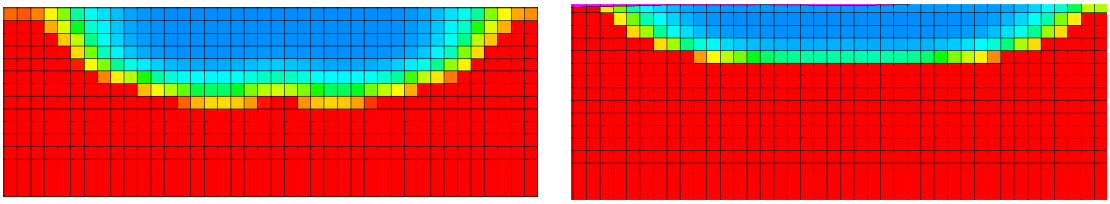

Figure 5.14: Movement of freshwater plume over time in different salinity profiles

Considering the recovery efficiencies in the aquifer with 650 ppm to 30,000ppm salinity profile, it can be concluded that ASR operation in such saline aquifer is not feasible. However the less saline aquifer has acceptable recovery efficiency over short storage periods.

From Figure 5.13 it is apparent that change in density difference ratio from 0.007 to 0.02 has a drastic impact on recovery efficiency for short time storage, while both conditions are unsuitable for long time storage scenarios.

Chapter 6

Conclusions

The Liwa aquifer storage and recovery project proves to be an excellent alternative source of fresh water in case of emergency situations for Emirate of Abu Dhabi, United Arab Emirates.

The affect of various operational and aquifer characteristic parameters on the recovery efficiency was studied.

The storage duration had a considerable impact on the recovery efficiency. It was observed that after 10 years of storage the recovery efficiency was reduced by 33%, and after 15 years only half of injected water was recoverable while the immediate recovery could produce almost the total injected water. It was also noticed that while the time has a linear relationship with recovery efficiency at the beginning, it tends to stabilize after certain time when the fresh water plume reached the surface and became steady.

The pumping rate though had a significant effect on the salinity on the discharged water at a certain time during recovery; it did not influence the recovery efficiency much, because of the presence of impermeable layer underneath and the low vertical hydraulic conductivity. However when a homogenous aquifer was simulated the upconing affect that led to the early termination of recovery was observed.

The shallower the screen location, the better recovery efficiency was observed until it reached an optimum value. Overall, the change in the screen location did not have a considerable impact on the recovery efficiency.

Multiple cycle operation improved the recovery efficiency greatly; just the second cycle improved the recovery efficiency by 33%. Also after 10 cycles the ASR was able to achieve a 100% recovery in spite of 1 year storage.

Additional one month recharge during the storage period noticeably increased the recovery efficiency; the rise in the recovery efficiency was much more visible with the longer storage periods.

In additional to the operational scenarios discussed the affect of dispersion and salinity profile on the recovery efficiency was also studied.

As expected the higher dispersion reduced the recovery efficiency. However, the longer storage periods tend to very much reduce this effect to the point that after certain storage duration the effect of dispersion could be neglected.

At last, the impact of salinity profile was proved to be very significant. Both aquifers with the density difference ratio of 0.007 and 0.02 were considered unsuitable for long time storage, while the less saline aquifer had acceptable performance for short time storage periods.

In conclusion, in order to make the Liwa ASR project a success, operational scenarios should be carefully designed, keeping the impact of each parameter in mind. In

order to have an acceptable performance for long storage periods, multiple cycle operation or additional recharge during storage or a combination of both should be considered.

References

Dawoud, M.A. (2010). Three Dimensional Geodatabase based Model for Groundwater Aquifer and Storage, Proceedings of the *7th International Symposium on Managed Aquifer Recharge*, Abu Dhabi, United Arab Emirates, October 9-13, 2010.

Esmail, O.J., Kimbler, O.K. (1967). Investigation of the Technical Feasibility of Storing Freshwater in Saline Aquifers. *Water Resources Research* 3 (3), 683-695.

Missimer, T.M., Guo, W., Walker, C.W., Maliva, R.G. (2002). Hydraulic and Density Considerations in the Design of Aquifer Storage and Recovery Systems. *Florida Water Resources Journal*, February, 31–35

Reilly T.E. & Goodman A.S. (1987). Analysis of Saltwater Beneath a Pumping Well. *Journal of Hydrology*, Vol. 89, PP 169–204.

Saeid, M.M., Bruen, M. (2004). Simulation of Hydrosalinity Behavior under Skimming Wells. *Irrigation and Drainage Systems*, Vol. 18, 167-200.

Ward, J.D., Simmons, C.T., Dillon, P.J. (2007). A Theoretical Analysis of Mixed Convection in Aquifer Storage and Recovery: How Important Are Density Effects? *Journal of Hydrology*, Vol. 343, PP. 169–186.

Ward, J.D., Simmons, C.T., Dillon, P.J. (2008). Variable-density Modeling of Multiple-cycle Aquifer Storage and recovery (ASR): Importance of Anisotropy and Layered Heterogeneity in Brackish Aquifers. *Journal of Hydrology*, Vol. 356, No. 93-105.

Wirojanagud, P., Charbeneau, R.J. (1985). Saltwater Upconing in Unconfined Aquifers. *Journal of Hydraulics Engineering*, Vol. 111, No. 3, PP. 417-434